On Mitigation of Sub-Synchronous Control Interactions in Hybrid Generation Resources

Farshid Salehi , *Member, IEEE*, Amir Golshani , *Member, IEEE*,
Igor Brandão Machado Matsuo , *Student Member, IEEE*, Payman Dehghanian , *Senior Member, IEEE*,
Mehriar Aghazadeh Tabrizi, *Member, IEEE*, and Wei-Jen Lee , *Fellow, IEEE*

Abstract—One major reliability concern regarding renewable energy resources connected in the vicinity of series-compensated power transmission lines or to weak power grids is subsynchronous resonance. A particular type of interaction known as subsynchronous control interaction (SSCI), with a purely electrical nature, has the potential to grow very rapidly and can cause severe damage to power grid infrastructure. This article proposes an additional damping controller that allows mitigating the SSCI expeditiously. The proposed damping loop provides a very large impedance at the synchronous frequency and very low impedance at the subsynchronous range. More importantly, it can be integrated into the control loop of the battery energy storage systems (BESS) without imposing a negative impact on the routine performance of the BESS. As BESSs are becoming more popular in power grids, thanks to their significant impacts on reliability and power quality, it is anticipated that the proposed approach will have a great implementation opportunity. Hence, the proposed mitigation solution is implemented in a hybrid plant and tested with a radial test system and a section of the Electric Reliability Council of Texas power grid under a variety of operating conditions. The results show the efficiency and robustness of the mitigation solution even under different frequencies of oscillation and larges disturbances.

Index Terms—Battery energy storage system (BESS), damping, hybrid generation resources, mitigation, subsynchronous control interaction (SSCI), subsynchronous resonance (SSR), wind farms.

I. INTRODUCTION

BATTERY energy storage systems (BESSs) provide numerous benefits in power systems including improvement of the voltage profile [1], peak shaving [2], provision of ancillary services, and improvement in reliability and power quality indices [3]. Specifically, BESS is a key contributor to developing a stable power grid that highly relies on intermittent energy sources. Nowadays, hybrid generation resources consisting of solar/wind plants and BESS are drawing more attention and new power plants are being developed based on this configuration [4]. The hybrid configuration, where multiple resources share one point of interconnection (POI), delivers a better generation profile, makes efficient use of the existing land, overcomes the inherent uncertainty of renewable resources, and provides a greater opportunity for energy arbitrage. As the penetration of intermittent energy sources grows, the role of BESS to improve power grid reliability becomes more crucial [3].

The widespread penetration of intermittent energy resources brings about challenging concerns related to subsynchronous control interactions (SSCIs), which is a relatively new reliability concern pertaining to renewable resources connected to weak grids or in the vicinity of series-compensated transmission lines [5]–[15]. Some types of subsynchronous resonance (SSR) phenomenon involve the torsional modes of the mechanical system; hence, the frequency of oscillation is fixed and the oscillation grows gradually [5], [7], [10]. However, SSCI is a particular type of interaction between the control system of wind/solar plants and the series-compensated power lines. The behavior depends on the operating conditions and the electrical parameters; hence, the frequency of oscillation can vary and the oscillation can grow rapidly—in the order of a few hundreds of milliseconds [10]. Due to these features, SSCI can lead to severe damage to power grid infrastructure such as wind/solar plants, series capacitors, and shunt elements [5]–[15].

Incidents of SSCI between type-3 wind farms and series-compensated transmission lines have been reported around the world [16], among which are: the 2007 south central Minnesota subsynchronous oscillation which caused damage to nearby buswork and some of the wind turbine components; the 20 Hz oscillations at the Electric Reliability Council of Texas (ERCOT) power grid in 2009 which resulted in damage to the series capacitors and wind turbine crowbar circuits; several 3–12 Hz oscillations in north China between 2012 and 2013, all involving

type-3 wind farms and series-compensated power transmission lines; and different events with 22–27 Hz oscillations in the ERCOT power grid in 2017 which did not cause any damage as all wind turbines were equipped with SSR mitigation options [6], [14]. Also, incidents of SSCI are reported when type-4 wind farms are connected to the weak grids in the northwest of China in 2015. The details of all above mentioned incident are elaborated in [16]. Following the ERCOT 2009 event, most system operators have developed protocols and instructions to mandate the implementation of SSCI mitigation or detection schemes in the case of any SSCI risk [10]. Therefore, different techniques have been proposed to mitigate SSCI risks. In the generation side, many researchers have tried to address this issue through a turbine/inverter-level solution involving the addition of a damping control loop or modification of an existing control loop to improve the subsynchronous damping capability of the turbine/inverter (see [14]–[23]). In [14], for example, a supplementary control loop for the grid-side converter of the doubly-fed induction generator (DFIG) only using the voltage across the series-capacitor as the input is used and demonstrated to be a simple, yet effective, mitigation solution. Analysis and mitigation of SSCI in DFIG systems with experimental validation is presented in [24] where it is concluded that the DFIG system can become immune to SSCI for any level of series compensation provided that the sensitive proportional parameters of the rotor-side converter are properly tuned. In [25], a subsynchronous oscillation suppression strategy for doubly-fed wind power generation systems based on harmonic current extractions is proposed for the frequency adaptability of the quasi-resonant controller. An effective voltage source converter (VSC) based control scheme, the so-called SSR dynamic suppressor, is suggested in [26] that is envisioned to be placed at the point of common coupling of the power plant for multi-generator SSR suppression purposes. An inertia phased-locked loop (PLL) is suggested in [27] to suppress the SSR caused by the impedance interaction between the renewable energy generation system and the weak grid. Impedance modeling and analysis for DFIG-based wind farms in SSO studies is researched in detail in [28], where the outer loop controller, PLL, and grid-side controller are all considered. The concept of motion-induction amplification is introduced in [29] and a new motion-induction compensation scheme is accordingly suggested as a solution to mitigate the SSO in wind farms connected to series-compensated transmission lines. A comparison of methods to examine SSR oscillations caused by grid-connected wind turbine generators is presented in [30]. The main challenge in implementing these approaches is having access to the intellectual property of the manufacturer models for the turbine/inverter, which is almost impossible, making these approaches impractical and infeasible for third parties. Moreover, these solutions may require not only rework for tuning the turbine/inverter parameters, but also shutting down the generators during implementation in the power plant, which sometimes has equipment from several different manufacturers. Baesmat and Bodson [31] demonstrated that the SSR problem in a DFIG connected to a series-compensated line is magnified when the stator alignment is used and, therefore, designed an observer that emulates the grid-alignment without requiring grid voltage measurements and proposed mechanisms

for SSR suppression through DFIG excitation control. In [32], a BESS with an additional loop using a power system stabilizer is used for SSR mitigation, but it is only applied to conventional units, which are slower than SSCI due to the mechanical nature of the interaction. Contrary to solutions on the generation side, some other literature have proposed grid-level solutions or balance of plant approach that consider the utilization of flexible ac transmission system devices or other active elements in the power grid to provide the necessary damping [33]–[38]. In [33], for example, a Kalman-filter-based mitigation scheme using a static-series-synchronous compensator is used to mitigate SSR. In [34], a mitigation solution based on a static synchronous compensator (STATCOM) is proposed which improves the stability of the system. Model-free adaptive control of STATCOM for SSO mitigation in DFIG-based wind farms is investigated in [39]. An enhancing grid stiffness control strategy of STATCOM/BESS for damping SSR in wind farms connected to weak grids is proposed and experimentally validated in [40]. A coordinated damping optimization control of SSR oscillations for DFIG and static var generator is proposed in [41]. A nonlinear SSR oscillation damping controller for direct-drive wind farms with VSC-HVdc systems is proposed and investigated in [42]. A systematic procedure to mitigate the interactions between a DFIG and a series compensated transmission line using the phase imbalance compensation (PIC) concept is proposed in [43], the performance of which was tested and validated under both series and parallel connection scenarios. Nevertheless, these methods are also featured with a few drawbacks. First, each solution relies on the specific device and availability of these elements in the section of the grid with SSCI risk. Second, these elements are typically owned by transmission providers, whereas the generation owner is responsible for providing an SSCI mitigation solution per some of the existing grid codes. Ownership and operation of the SSCI mitigation by one stakeholder while another stakeholder faces the risks and responsibilities create more complexity and could render the grid reliable operation impractical.

This article aims to address the above-mentioned drawbacks associated with the existing inverter/turbine-level and grid-level solutions while providing mitigation at the generation-side (often responsible to provide SSCI mitigation solutions) with the use of an existing BESS. Moreover, it aims to maximize the benefits of the BESS used in a hybrid configuration with solar/wind resources. Additionally, we extend a patent of DNV in an application that introduces a new function for the existing BESS in hybrid plants besides the major ones extensively discussed in the literature [44]. Under this new approach, by modifying the active/reactive power controller and accommodating a supplementary control loop, the existing BESS will also be an active participant in damping the SSCI events. Note that the supplementary control loop will not influence the normal operation of BESS, as it only comes into effect when an SSCI event is detected. To this end, a filter-less damping controller has been designed whose output signal is fed forward into the control loops of the BESS. This approach uses the terminal voltage of the BESS as the input signal to the damping loop without having to utilize any band-pass or high-pass filters. In fact, the proposed approach is an active device that provides low and high
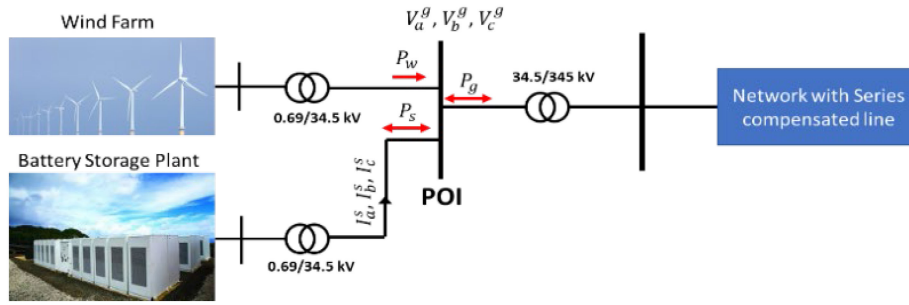
Fig. 1.   One-line diagram of a hybrid energy system connected to a series-compensated power transmission line.
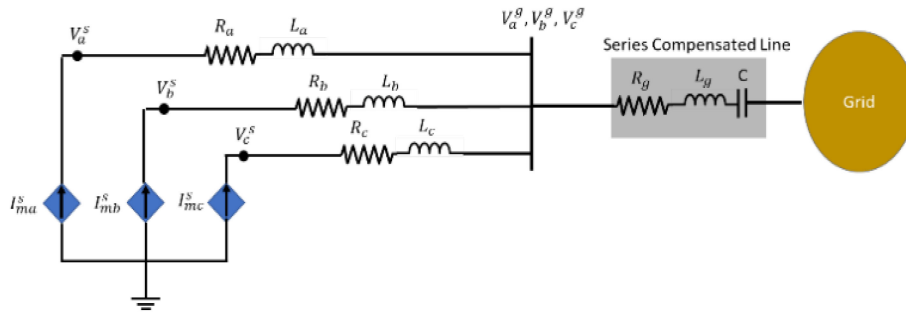

Fig. 2.   Battery storage plant represented by an average model of the current source inverter.

impedances for the subharmonic and fundamental frequencies, respectively.

The proposed mitigation method considers some of the most important practical factors to design a feasible SSCI mitigation countermeasure [8], [44]. The main contributions and features can then be summarized as follows: the proposed method is independent of the turbine/inverter technology and can be simply implemented by third parties; herein, it is implemented using a BESS. However, the idea is generic enough to be implemented on any active element which can be a source of energy; its design does not involve any filtering, which overcomes the issue that different oscillation frequencies may appear in different operating conditions and electrical parameters, making it more accurate and flexible for any range of SSCI frequencies; it is always in service without affecting the power frequency in normal operating conditions; it carefully selects a damping signal that will work for the whole hybrid plant, instead of only for individual wind turbines or solar units; and it has the capability to mitigate oscillations under different operating conditions, such as different power plant dispatch levels and system configurations, while damping SSCI under both small and large disturbances in the power grid, having been extensively evaluated using an actual ERCOT power grid data set.

The rest of this artticle is organized as follows. Section II introduces the proposed damping controller along with the mathematical formulations. Section III examines the performance of the damping controller under a radial test grid and a section of the ERCOT power grid using frequency scanning, eigenvalue analysis and time-domain electromagnetic transient (EMT) simulations. Finally, Section IV concludes this article.
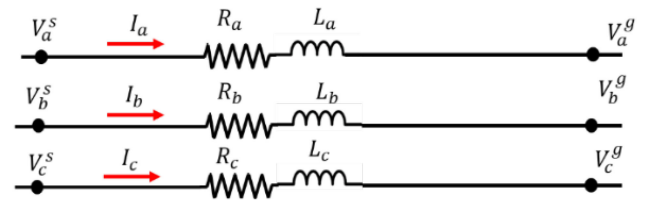

Fig. 3.   Three-phase RL circuit.

II. DESIGN AND IMPLEMENTATION OF THE DAMPING CONTROLLER

In this section, we introduce the proposed SSCI mitigation approach and present a detailed model of the damping controller. Fig. 1 illustrates a hybrid energy system where a large-scale wind farm shares a POI with a BESS. In normal operation, the BESS can provide bidirectional active power flow, counteracting wind power fluctuations. The equivalent network shown in Fig. 2 represents an average model of a BESS connected to a bulk power system via a series-compensated transmission line. Current sources I_{ma}^s, I_{mb}^s, and I_{mc}^s are derived from Fig. 3, and $R_a = R_s + R_D$ and $L_a = L_s + L_D$. Note that R_D and L_D represent the virtual damping resistor and inductor, respectively. In fact, the damping resistor and inductor do not exist physically, and they come into effect only for subsynchronous frequencies.

Fig. 4 shows the proposed BESS controller envisioned to be capable of an efficient SSCI damping. In normal operation, the active and reactive power settings are provided by the supervisory control and the proposed controller follows
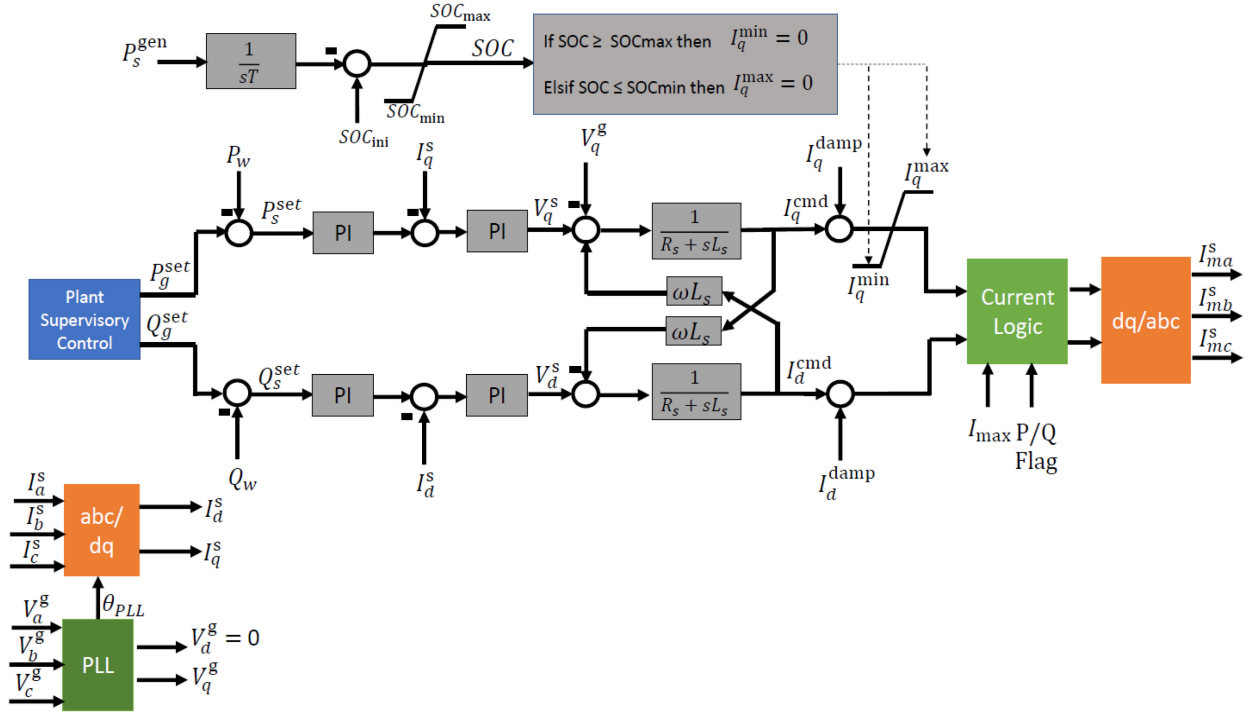
Fig. 4. Proposed controller for the battery storage plant with SSCI damping capability.

the desired set-point. In this case, I_q^{cmd} is proportional to the active power and I_d^{cmd} is proportional to the reactive power. No damping current is required during normal operation (i.e., $I_q^{\text{damp}} = 0$ and $I_d^{\text{damp}} = 0$). In case of an SSCI event, an additional signal is incorporated in the proposed controller in a feed-forward fashion that is meant to mitigate the oscillation in wind power plants. Here, we further elaborate on the structure of the damping controller by deriving a set of equations generating the I_q^{damp} and I_d^{damp} signals.

The idea behind the damping signal is to insert a small virtual shunt impedance between the wind farm and the series-compensated transmission line, presenting a low impedance in the entire subsynchronous frequency range and the high impedance at the nominal 60 Hz frequency. Fig. 3 shows an RL circuit connected between two sources V_a^s and V_a^g. The equations of such circuit can be written as presented in [8]

$$V_{a,b,c}^s - V_{a,b,c}^g = R_{a,b,c} I_{a,b,c} + L_{a,b,c} \frac{dI_{a,b,c}}{dt}. \quad (1)$$

Assuming $R_a = R_b = R_c = R_s$ and $L_a = L_b = L_c = L_s$, and after transforming (1) into *dq0* frame, we obtain

$$V_q^s - V_q^g = R_s I_q + L_s \frac{dI_q}{dt} + \omega L_s I_d$$

$$V_d^s - V_d^g = R_s I_d + L_s \frac{dI_d}{dt} - \omega L_s I_q$$

$$V_0^s - V_0^g = R_s I_0 + L_s \frac{dI_0}{dt}. \quad (2)$$

In (2), subscripts "*d*," "*q*," and "0" represent the quadrature, direct, and zero terms of the terminal voltages, and ω denotes the angular speed. Applying the Laplace transform, (2) can be

written as

$$V_q^s(s) - V_q^g(s) = R_s I_q(s) + L_s s I_q(s) + \omega L_s I_d(s)$$

$$V_d^s(s) - V_d^g(s) = R_s I_d(s) + L_s s I_d(s) - \omega L_s I_q(s)$$

$$V_0^s(s) - V_0^g(s) = R_s I_0(s) + L_s s I_0(s). \quad (3)$$

By rearranging (3), one can obtain the quadrature term of the current as

$$I_q(s) = \frac{(R_s + L_s s)\left(V_q^s(s) - V_q^g(s)\right) - \omega L_s\left(V_d^s(s) - V_d^g(s)\right)}{(R_s + L_s s)^2 + (\omega L_s)^2}. \quad (4)$$

Similarly, $I_d(s)$ can be written as

$$I_d(s) = \frac{\omega L_s\left(V_q^s(s) - V_q^g(s)\right) + (R_s + L_s s)\left(V_d^s(s) - V_d^g(s)\right)}{(R_s + L_s s)^2 + (\omega L_s)^2}. \quad (5)$$

According to (4) and (5), one can observe that the quadrature and direct terms of the currents in an RL circuit can be related to their respective voltages by two-second-order transfer functions. In other words, injecting $I_q(s)$ and $I_d(s)$ at a specific bus would mimic an RL circuit connected to that bus. That being said, the same idea can be adopted to design an adjustable RL circuit by the injection of variable current sources into a bus. The proposed damping controller inserts a virtual resistance and inductance with which the SSCI phenomenon can be mitigated.

The damping controller can be realized using equations (6) and (7) shown at the bottom of next page. We can observe that
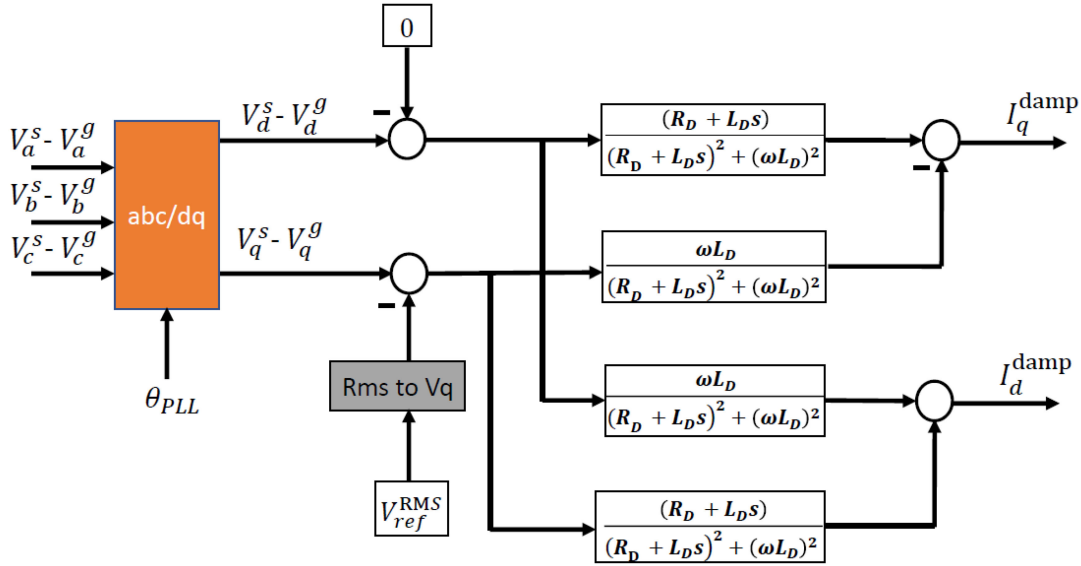
Fig. 5.   Proposed damping controller to generate the feedforward term.

the injection of the damping currents $I_q^{\text{damp}}(s)$ and $I_d^{\text{damp}}(s)$ are equivalent to inserting a virtual impedance in the network. However, one should note that the virtual impedance must not be in effect for the fundamental frequency (60 Hz). In this way, the damping controller should be designed in a way that the injected damping currents become zero for the fundamental frequency. To satisfy this condition, we proposed the SSCI damping controller as presented in Fig. 5. Having the grid voltage aligned with the q-axis, the direct axis voltage $V_d = 0$ and the quadrature component V_q becomes a constant value at the fundamental frequency. Therefore, by eliminating the dc component of V_q, the injected damping current at the fundamental frequency becomes zero. Equivalently, the virtual impedance will be eliminated from the current path. It should be noted that the dc component can also be eliminated using a high-pass filter; however, it adds a phase shift that would affect the performance of the damping controller

It should be noted that the proposed solution monitors the voltage at the POI for the hybrid generation and acts as a countermeasure to mitigate the SSCI risk of the renewable portion; therefore, it should be considered as a standalone solution for hybrid generation and not a grid solution. Additionally, since the damping controller is implemented as a feedforward loop, it is expected to have a minimal impact on the BESS control system. However, to implement this mitigation option in practice, it is recommended to revisit all the limits and ramp rate specific to each project and condition to ensure the effectiveness and robustness of the SSCI mitigation without any adverse impact on the normal performance of the BESS.

III. SIMULATION AND NUMERICAL RESULTS

In this section, the proposed solution is implemented in a hybrid plant consisting of a 100 MW DFIG-based wind farm and a 30 MW BESS system. The performance of the mitigation system is tested utilizing the frequency-scan-based technique, eigenvalue analysis, and detailed time-domain EMT simulations. Due to the limitations and complexity of access to the manufacturer-specific equipment, hardware-in-the-loop simulations are not part of this article. Time-domain EMT simulation was used herein, which is the most common and effective technique for the validation of SSCI-phenomenon-related systems by many power grid operators. A case connecting the hybrid plant to a radial test system as well as a case where it is connected to an ERCOT power grid section are tested and analyzed.

A. Radial Test Case

In the radial test case, the hybrid plant is connected to an equivalent grid by a series-compensated line. The configuration of this case study is depicted in Fig. 1 and the parameters of the radial test cases are given in [8]. First, the harmonic-injection-frequency-scanning technique along with EMT simulations are employed to perform a detailed SSCI analysis to assess the vulnerability of the system to the SSCI. This approach runs a separate frequency scan on the wind farm and the power grid to calculate the resistance and reactance of the wind farm and the grid for the entire subsynchronous frequency range. Then, both the wind-farm side and the grid side frequency scan results are used to estimate the cumulative resistance and reactance

$$I_q(s) + I_q^{\text{damp}}(s) = \frac{(R_s + R_D + (L_s + L_D)s)\left(V_q^s(s) - V_q^g(s)\right) - \omega(L_s + L_D)\left(V_d^s(s) - V_d^g(s)\right)}{(R_s + R_D + (L_s + L_D)s)^2 + (\omega(L_s + L_D))^2} \tag{6}$$

$$I_q(s) + I_d^{\text{damp}}(s) = \frac{\omega(L_s + L_D)\left(V_q^s(s) - V_q^g(s)\right) + (R_s + R_D + (L_s + L_D)s)\left(V_d^s(s) - V_d^g(s)\right)}{(R_s + R_D + (L_s + L_D)s)^2 + (\omega(L_s + L_D))^2} \tag{7}$$
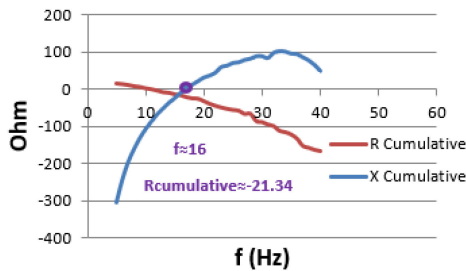
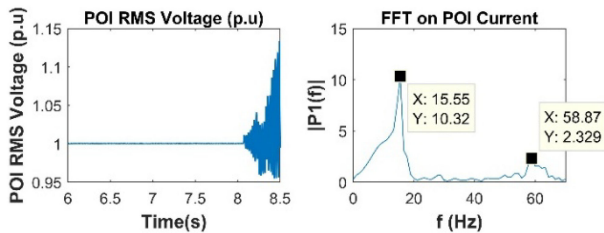Fig. 6. Frequency scan results (cumulative resistance and reactance); battery in ideal mode; without damping loop.

Fig. 7. EMT results for the scenario of battery storage in ideal mode and without the damping loop.

TABLE I
FREQUENCY SCAN RESULTS: RADIAL TEST CASE WITH MITIGATION

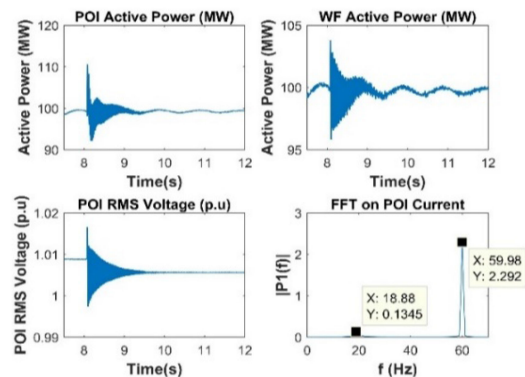| Wind Farm Operating Condition	BESS	Cross-over Frequency (Hz)	Cumulative Resistance (Ohm)	SSCI Risk
100% turbines at 100% dispatch	Ideal	19	1.83	No
	Charging	19	1.07	No
	Discharging	19	3.67	No

Fig. 8. Radial test system with damping loop; BESS in ideal mode.

Fig. 9. Radial test system with damping loop; BESS in charging mode.

over the subsynchronous range. The cumulative resistance at the cross-over frequency (zero-reactance frequency) is the quantitative index representing the SSCI risk [6]. A negative or zero resistance at this resonant frequency indicates the SSCI risk. The details of the SSCI analysis and the relation of the damping capability with resistance are elaborated in [7], [10], and [15]. In this article, the SSCI risk analysis is performed in two different conditions of the radial test case: the BESS does not have the damping loop and the BESS is equipped with the damping loop.

1) Radial Test Case Without the Damping Loop: In this scenario, the hybrid generation unit does not have the damping controller loop and the BESS is in ideal mode, meaning it is neither charging nor discharging. The results of the frequency scan (cumulative resistance and reactance) for this scenario are depicted in Fig. 6. As can be seen in this plot, the cross-over frequency (purple dot) is approximately around 16 Hz, at which there is a negative cumulative resistance of approximately -21.34 Ω, which indicates the SSCI risk.

A detailed EMT simulation is performed to validate the frequency-scan outcome. For the EMT simulation, firstly, the series capacitor is bypassed by a switch and the simulation is executed until $t = 8.065$ s to make sure that the system is in a steady-state condition. At $t = 8.065$ s, the bypass switch is opened and a radial connection with the series-compensated line occurs. The results including the RMS voltage at the POI and the fast Fourier transform (FFT) of the POI current are depicted in Fig. 7. As expected, the results confirm the existence of SSCI at the estimated frequency.

2) Radial Test Case With the Damping Loop: In this scenario, the damping controller loop is implemented in the battery storage control system and the radial connection of a hybrid plant is tested under various operation modes of the BESS (ideal, charging and discharging). The frequency-scan results for these scenarios are given in Table I. The results show that the addition

of the damping loop can shift the resonant frequency from 16 to 19 Hz and lead to a positive cumulative resistance at this resonance frequency.

The EMT simulation is performed for all scenarios as illustrative examples, the results for ideal and charging mode are depicted in Figs. 8 and 9. As it can be seen, the addition of the proposed damping controller can efficiently mitigate the SSCI. It should be noted that since the battery storage control loop does not vary under different operating modes and the damping loop is added as a feedforward term, the BESS mode of operation does not affect the performance of the proposed damping method.

B. ERCOT Test Case

In this test case, the wind farm and battery storage are connected to a section of the ERCOT power grid with high penetration of wind resources while exporting the power through a series-compensated line. The overall structure of this area, which is a combination of wind generation and series-compensated lines, increases the risk of SSCI. The ERCOT grid section is depicted in Fig. 10. A hybrid generation resource comprising a
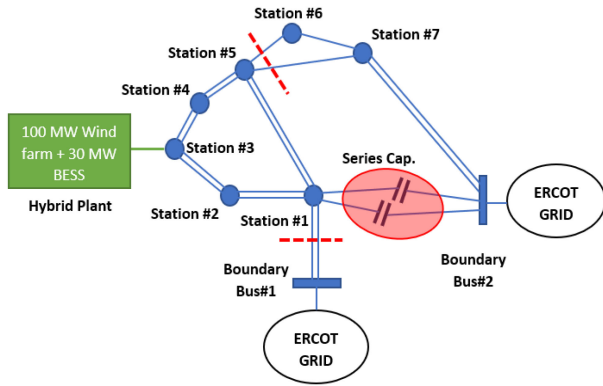
Fig. 10. ERCOT power grid section with series-compensated lines.

TABLE II
N-4 CONTINGENCY DEFINITION

Item	Element	From	To	Circuit #
1	Transmission Line	Station #5	Station #6	Circuit #1
2	Transmission Line	Station #5	Station #7	Circuit #1
3	Transmission Line	Station #1	Boundary Bus#1	Circuit #1
4	Transmission Line	Station #1	Boundary Bus#1	Circuit #2

100 MW wind farm and a 30 MW battery storage is connected to substation #3 (POI).

Based on the topology check, the minimum contingency rank that results in a radial connection between the hybrid plant and the series-compensated line is N-4. This contingency involves the opening/tripping of the lines given in Table II. Similar to the radial test case, the SSCI analysis is performed for the hybrid plant with and without the damping loop.

1) ERCOT Test Case Without Damping Loop: The purpose of analyzing this scenario is to perform an SSCI vulnerability assessment for the interconnection of the wind farm to this section of the ERCOT power grid. This involves performing an SSCI risk assessment under different operating conditions of the wind farm and the power grid. To accomplish a wide-range SSCI vulnerability assessment, the following scenarios of wind farm operation are considered;.

1) *Normal Operation:* 100% of the turbines are online and in full (100%) dispatch.
2) *Minimum Dispatch:* 100% of the turbines are online and in minimum dispatch, which in this case is 20%. This scenario simulates a wind drop condition in the field.
3) *Minimum Number of Turbines:* 20% of the turbines are online and in full (100%) dispatch. This scenario simulates the start-up of the wind farm in the field.

For the transmission side, the status of critical shunts in the transmission grid is studied to account for different power grid operating conditions. A switch shunt is assumed to be critical if its location lies between the POI and the series-compensated line. For each of the three wind-farm scenarios above, this article considered the grid with all or none of the critical shunt elements in operation. In this way, we can study the variation of the expected subsynchronous frequency range for different operating conditions of the grid as well. The final scenarios are then defined as in Table III. The compensation level is fixed at

TABLE III
SCENARIOS WITH VARIOUS WIND-FARM AND GRID OPERATING CONDITIONS

Scenario	WF Operating Condition	Grid Operating Condition
SC1	100% turbines at 100% dispatch	No Shunts
SC2	100% turbines at 100% dispatch	All Shunts
SC3	100% turbines at 20% dispatch	No Shunts
SC4	100% turbines at 20% dispatch	All Shunts
SC5	20% turbines at 100% dispatch	No Shunts
SC6	20% turbines at 100% dispatch	All Shunts

TABLE IV
FREQUENCY SCAN RESULTS WITHOUT DAMPING LOOP

Scenario	SSCI Freq. (Hz)	Cumulative R (Ohm)	SSCI Risk
SC1	10	-6.35	Yes
SC2	14	-13.15	Yes
SC3	10	-11.2	Yes
SC4	14	-20.76	Yes
SC5	6	0.27	No
SC6	12	-85.92	Yes

TABLE V
EIGENVALUE RESULTS WITHOUT DAMPING LOOP

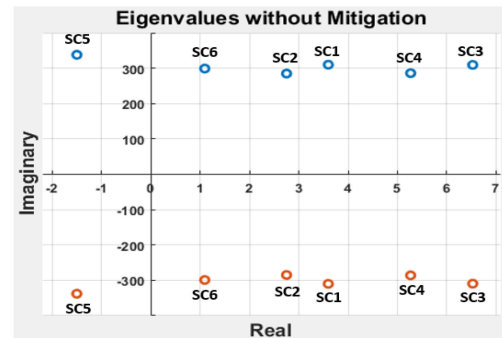| Scenario	SSCI Freq. (Hz)	Real	Imaginary	SSCI Risk
SC1	10.7	3.60	309.85	Yes
SC2	14.7	2.75	284.84	Yes
SC3	10.8	6.53	309.38	Yes
SC4	14.5	5.27	285.98	Yes
SC5	6.2	-1.50	337.85	No
SC6	12.4	1.09	298.97	Yes

Fig. 11. Eigenvalue loci for all scenarios without damping loop.

50%; thus, it is not required to perform any sensitivity analysis around the compensation level of the series capacitor.

The harmonic injection frequency-scan based screening results for all scenarios are given in Table IV. We can see that, for all scenarios except scenario SC5, there is negative damping at the subsynchronous resonant (cross-over) frequency, which implies a high risk of SSCI at these frequencies and a need for SSCI mitigation. The eigenvalue analysis was also performed and the results corresponding to all scenarios are given in Table V with the locus of each eigenvalue is shown in Fig. 11.

We can see that all scenarios except for SC5 show a positive real part of the eigenvalue (eigenvalues are on the right-hand side of the real-imaginary plane), which means the system is not stable at these frequencies and can result in unstable SSCI oscillation. This is in accordance with the frequency scan results. It is important to recall that due to the *d–q* reference
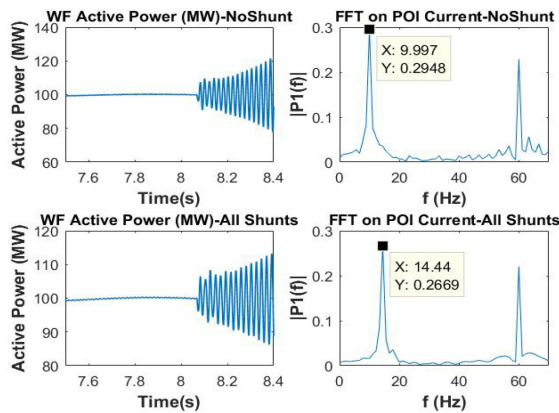
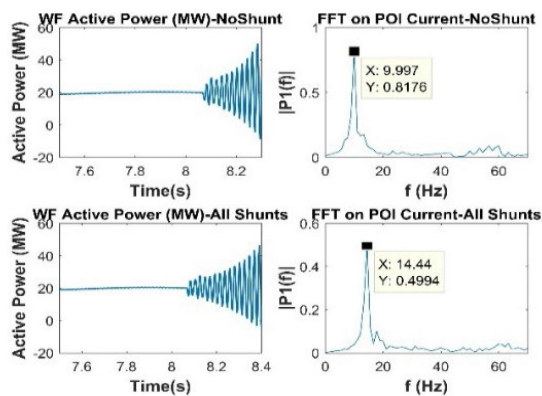Fig. 12. EMT simulation results for 100% turbines at 100% dispatch.

Fig. 13. EMT simulation results for 100% turbines at 20% dispatch.

TABLE VI
FREQUENCY SCAN RESULTS WITH DAMPING LOOP

Scenario	SSCI Freq. (Hz)	Cumulative R (Ohm)	SSCI Risk
SC1	12	5.93	No
SC2	15	8.04	No
SC3	11	4.2	No
SC4	15	6.23	No
SC5	10	22.73	No
SC6	14	29.58	No

TABLE VII
EIGENVALUE RESULTS WITH DAMPING LOOP

Scenario	SSCI Freq. (Hz)	Real	Imaginary	SSCI Risk
SC1	11.9	-3.65	302.00	No
SC2	15.5	-3.18	279.90	No
SC3	11.6	-1.88	303.92	No
SC4	15.2	-2.45	281.41	No
SC5	10.8	-12.48	309.26	No
SC6	14.6	-8.70	285.38	No
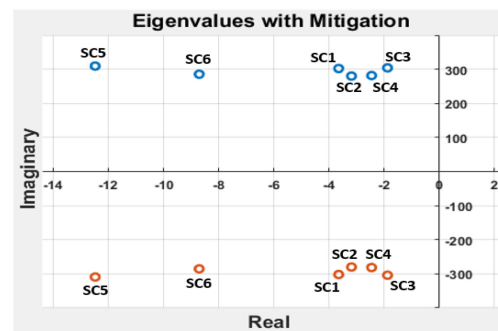
Fig. 14. Eigenvalue loci for all scenarios with damping loop.

frame, modes contain the complementary-to-the-fundamental frequency for the SSCI [10].

Finally, time-domain EMT simulations are performed for all operating conditions to corroborate the results of all previous analyses. Herein, the radial condition happens at $t = 8.065$ s. The details of the EMT simulation steps are elaborated in [10].

The wind-farm active power output and FFT results on the POI current for SC1 to SC4 are depicted in Figs. 12 and 13. In line with the frequency-scan screening and eigenvalue analysis, the EMT plots also show the existence of growing SSCI oscillations in all scenarios, except scenario SC5, and the oscillation frequencies calculated by the FFT analysis closely match the frequency scan and the eigenvalue results.

2) ERCOT Test Case With Damping Loop: The analysis presented in the previous section proved that under the *N*-4 contingency, the wind plant is prone to SSCI under different operating conditions. Therefore, there is an urgent need for a mitigation or detection solution. The proposed damping controller loop was added to the existing BESS system and the SSCI analysis was repeated. The results of the frequency scan are given in Table VI.

The eigenvalue results for all scenarios with the presence of the mitigation scheme are also given in Table VII and the locus of each eigenvalue is shown in Fig. 14. It is assumed that, while the wind farm is operating at full capacity, the battery is in charging mode of operation. However, when the wind farm is at minimum dispatch or with the minimum number of turbines in operation,

the battery is in discharging mode to compensate for the lack of the wind farm power.

The following discussion can be made around the results.

1) Addition of the proposed damping loop to the BESS results in a positive cumulative resistance at the SSCI frequencies. Thus, the hybrid plant has the capability to provide a positive damping at the SSCI frequency for all operating conditions, that is, the risk of SSCI has been mitigated effectively. The same conclusion can be reached from the eigenvalue analysis.

2) Addition of the damping loop can affect both the resonant frequency and its corresponding damping. It should be noted that the frequency shift for the ERCOT case is less than that for the radial test case. This is due to the interconnected nature of the large ERCOT grid.

To further evaluate the effectiveness of the proposed method, EMT simulation was performed for all scenarios and the results are indicative of a successful and expeditious damping of the SSCI within the ERCOT power grid. Due to space limitation, only the EMT plots for the normal operating scenarios (100% of turbines at 100% dispatch) are shown, in which the battery is in charging mode and all the critical shunts are out of or in service, as depicted in Figs. 15 and 16, respectively. Each plot involves the active power output of the wind farm, active power at the POI (summation of the wind farm and BESS outputs),
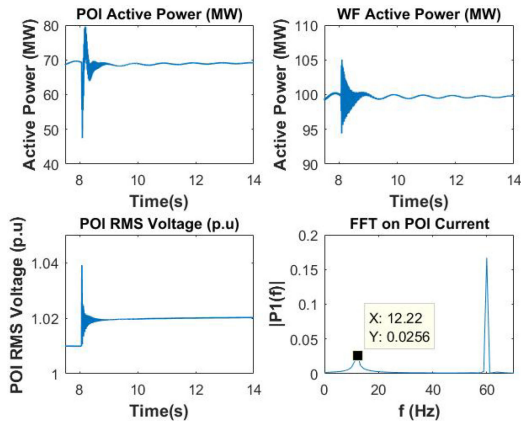
Fig. 15. No-fault scenario: 100% turbines at 100% dispatch; no shunts in service; and BESS in charging mode.
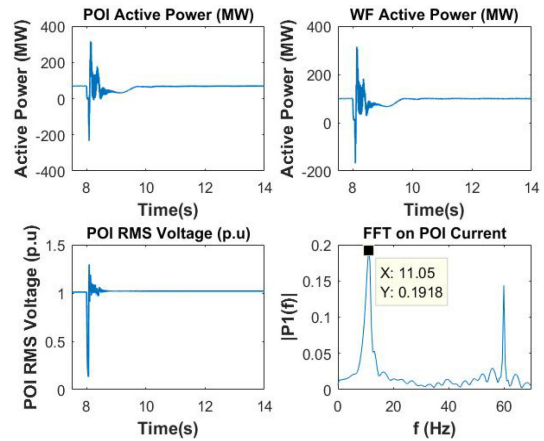

Fig. 17. Fault-based scenario: 100% turbines at 100% dispatch; no shunts in service; and BESS in charging mode.
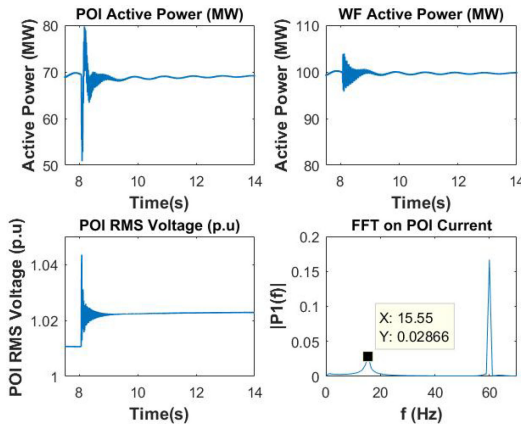

Fig. 16. No-fault scenario: 100% turbines at 100% dispatch; all shunts in service; and BESS in charging mode.
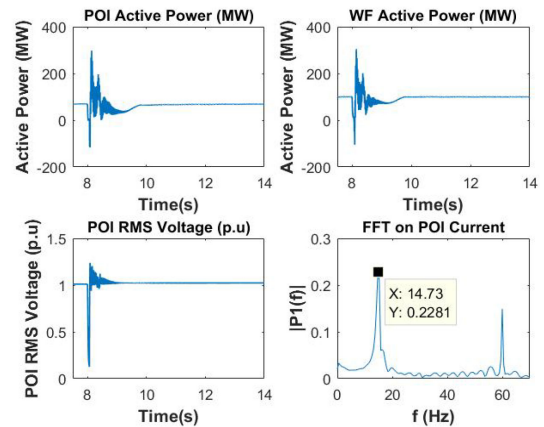

Fig. 18. Fault-based scenario: 100% turbines at 100% dispatch; all shunts in service; and BESS in charging mode.

rms voltage at the POI, and FFT results of the POI current. The following discussions can be made around the EMT simulation results.

1) For all scenarios, the proposed solution effectively damps the SSCI within almost one (1) second after the radial connection (at $t = 8.065$ s) and the system reaches steady state quickly;

2) These scenarios simulate the outage of double-circuit lines between Substation #1 and Boundary Bus #1 at $t = 8.065$ s to create a radial condition, as per the contingency definition. Thus, there is a 0.01 p.u. voltage jump related to the topology change in the transmission grid;

3) The frequency of the oscillation again closely matches the frequency scan and eigenvalue results.

3) Performance Under a Fault-Based Condition: In this section, a solid three-phase-to-ground fault is applied in the proximity of the POI at $t = 8$ s. The transmission lines between substation #1 and boundary bus #1 are tripped within four cycles. This condition is simulated to demonstrate the ability of the proposed solution to damp the SSCI under disturbances. The EMT results for both scenarios of no shunts and all shunts with the wind farm at 100% dispatch and with 100% of the turbines online are depicted in Figs. 17 and 18. It should be noted that the

battery is in charging mode in these operating scenarios; hence, the active power at the POI is lower than the wind farm capacity. The following observations can be reported on the fault-based scenario.

1) The severe fault close to the POI leads to a voltage dip during the fault and a high transient overvoltage at the POI following the fault clearance.

2) As it is evident from the active-power plots and the FFT magnitudes, the fault-based situation leads to more severe SSCI oscillations when compared to the no-fault condition.

3) Utilization of the voltage as the input signal for the damping control loop always raises concerns about the robustness of the solution under severe faults, as it may cause large voltage distortions. However, the results show that, even under large voltage disturbances, the proposed mitigation can still damp the oscillation within one second (similar to the no-fault condition).

IV. CONCLUSION

An advanced and robust mitigation solution was proposed to effectively damp subsynchronous oscillations in

wind-integrated power grids. The proposed technique was independent of turbine/inverter control schemes and does not had any impact on the power frequency during normal power grid operation. More importantly, the proposed method maximizes the benefits associated with hybrid BESS and wind/solar plants, although it provides the flexibility to be used with other active elements that was a source of energy. Moreover, its filter-less nature provides the capability of working throughout the subsynchronous range even under different operating conditions and grid configurations. The proposed damping controller was implemented in the BESS control system inside a hybrid power plant and was evaluated using both a radial test case and a section of the ERCOT power grid with series-compensated lines. Frequency scanning, eigenvalue analysis, and time-domain EMT simulations verified that the proposed solution can effectively damp the SSCI events under various operating conditions in the power grid, including large disturbances, which confirms its robustness.

Future research direction could be targeted toward mechanisms to quantify and evaluate how damping controller would affect the lifespan and useful capacity of the BESS. Additionally, financial mechanisms for BESS owners in providing SSCI mitigation and other ancillary services could be further researched.

REFERENCES

[1] M. N. Kabir, Y. Mishra, G. Ledwich, Z. Y. Dong, and K. P. Wong, "Coordinated control of grid-connected photovoltaic reactive power and battery energy storage systems to improve the voltage profile of a residential distribution feeder," *IEEE Trans. Ind. Informat.*, vol. 10, no. 2, pp. 967–977, May 2014.

[2] Y. Shi, B. Xu, D. Wang, and B. Zhang, "Using battery storage for peak shaving and frequency regulation: Joint optimization for superlinear gains," *IEEE Trans. Power Syst.*, vol. 33, no. 3, pp. 2882–2894, May 2018.

[3] W. Kim, J. Shin, and J. Kim, "Operation strategy of multi-energy storage system for ancillary services," *IEEE Trans. Power Syst.*, vol. 32, no. 6, pp. 4409–4417, Nov. 2017.

[4] T. Hirose and H. Matsuo, "Standalone hybrid wind-solar power generation system applying dump power control without dump load," *IEEE Tran. Ind. Electron.*, vol. 59, no. 2, pp. 988–997, Feb. 2012.

[5] A. E. Leon and J. A. Solsona, "Sub-synchronous interaction damping control for DFIG wind turbines," *IEEE Trans. Power Syst.*, vol. 30, no. 1, pp. 419–428, Jan. 2015.

[6] I. B. M. Matsuo, F. Salehi, L. Zhao, Y. Zhou, and W. Lee, "Optimized frequency scanning of nonlinear devices applied to sub-synchronous resonance screening," *IEEE Trans. Ind. Appl.*, vol. 56, no. 3, pp. 2281–2291, May/Jun. 2020.

[7] L. Fan, R. Kavasseri, Z. L. Miao, and C. Zhu, "Modeling of DFIG-Based wind farms for SSR analysis," *IEEE Trans. Power Del.*, vol. 25, no. 4, pp. 2073–2082, Oct. 2010.

[8] H. K. Nia, F. Salehi, M. Sahni, N. Karnik, and H. Yin, "A filter-less robust controller for damping SSCI oscillations in wind power plants," in *Proc. IEEE Power Energy Soc. Gen. Meeting*, 2017, pp. 1–5.

[9] Z. Miao, "Impedance-model-based SSR analysis for type 3 wind generator and series-compensated network," *IEEE Trans. Energy Convers.*, vol. 27, no. 4, pp. 984–991, Dec. 2012.

[10] F. Salehi, I. B. M. Matsuo, A. Brahman, M. A. Tabrizi, and W. Lee, "Subsynchronous control interaction detection: A real-time application," *IEEE Trans. Power Del.*, vol. 35, no. 1, pp. 106–116, Feb. 2020.

[11] L. Wang, X. Xie, Q. Jiang, H. Liu, Y. Li, and H. Liu, "Investigation of SSR in practical DFIG-Based wind farms connected to a series-compensated power system," *IEEE Trans. Power Syst.*, vol. 30, no. 5, pp. 2772–2779, Sep. 2015.

[12] W. Du, Q. Fu, and H. Wang, "Method of open-loop modal analysis for examining the subsynchronous interactions introduced by VSC control in an MTDC/AC system," *IEEE Trans. Power Del.*, vol. 33, no. 2, pp. 840–850, Apr. 2018.

[13] W. Du, C. Chen, and H. Wang, "Subsynchronous interactions induced by DFIGs in power systems without series compensated lines," *IEEE Trans. Sustain. Energy*, vol. 9, no. 3, pp. 1275–1284, Jul. 2018.

[14] Y. Li, L. Fan, and Z. Miao, "Replicating real-world wind farm SSR events," *IEEE Trans. Power Del.*, vol. 35, no. 1, pp. 339–348, Feb. 2020.

[15] A. E. Leon, "Integration of DFIG-Based wind farms into series-compensated transmission systems," *IEEE Trans. Sustain. Energy*, vol. 7, no. 2, pp. 451–460, Apr. 2016.

[16] J. Rose *et al.*, "Wind energy systems sub-synchronous oscillations: Events and modeling," Tech. Rep. PES-TR80, pp. 1–155, Jul. 2020. [Online]. Available: https://resourcecenter.ieee-pes.org/publications/technical-reports/PES_TP_TR80_AMPS_WSSO_070920.html

[17] C. Karunanayake, J. Ravishankar, and Z. Y. Dong, "Nonlinear SSR damping controller for DFIG based wind generators interfaced to series compensated transmission systems," *IEEE Trans. Power Syst.*, vol. 35, no. 2, pp. 1156–1165, Mar. 2020.

[18] U. Karaagac, S. O. Faried, J. Mahseredjian, and A. Edris, "Coordinated control of wind energy conversion systems for mitigating subsynchronous interaction in DFIG-Based wind farms," *IEEE Trans. Smart Grid*, vol. 5, no. 5, pp. 2440–2449, Sep. 2014.

[19] H. A. Mohammadpour, A. Ghaderi, H. Mohammadpour, and E. Santi, "SSR damping in wind farms using observed-state feedback control of DFIG converters," *Elect. Power Syst. Res.*, vol. 123, pp. 57–66, 2015.

[20] P. Li, J. Wang, F. Wu, and H. Li, "Nonlinear controller based on state feedback linearization for series-compensated DFIG-based wind power plants to mitigate sub-synchronous control interaction," *Int. Trans. Elect. Energy Syst.*, vol. 29, no. 1, 2019, Art. no. e2682.

[21] M. A. Chowdhury and G. M. Shafiullah, "SSR mitigation of series-compensated DFIG wind farms by a nonlinear damping controller using partial feedback linearization," *IEEE Trans. Power Syst.*, vol. 33, no. 3, pp. 2528–2538, May 2018.

[22] X. Zhang, X. Xie, J. Shair, H. Liu, Y. Li, and Y. Li, "A Grid-side subsynchronous damping controller to mitigate unstable SSCI and its Hardware-in-the-loop tests," *IEEE Trans. Sustain. Energy*, vol. 11, no. 3, pp. 1548–1558, Jul. 2020.

[23] R. K. Varma and R. Salehi, "SSR mitigation with a new control of PV solar farm as STATCOM (PV-STATCOM)," *IEEE Trans. Sustain. Energy*, vol. 8, no. 4, pp. 1473–1483, Oct. 2017.

[24] M. T. Ali, D. Zhou, Y. Song, M. Ghandhari, L. Harnefors, and F. Blaabjerg, "Analysis and mitigation of SSCI in DFIG systems with experimental validation," *IEEE Trans. Energy Convers.*, vol. 35, no. 2, pp. 714–723, Jun. 2020.

[25] F. Meng, D. Sun, K. Zhou, J. Wu, F. Zhao, and L. Sun, "A sub-synchronous oscillation suppression strategy for doubly fed wind power generation system," *IEEE Access*, vol. 9, pp. 83482–83498, 2021.

[26] X. Yuan *et al.*, "An effective control scheme for multimodal SSR suppression via VSC-Based controller," *IEEE Access*, vol. 8, pp. 172581–172592, 2020.

[27] G. Li, Y. Chen, A. Luo, and Y. Wang, "An inertia phase locked loop for suppressing sub-synchronous resonance of renewable energy generation system under weak grid," *IEEE Trans. Power Syst.*, vol. 36, no. 5, pp. 4621–4631, Sep. 2021.

[28] P. Ju, B. Sun, M. Shahidehpour, and X. Pan, "Impedance modeling and analysis for DFIG-Based wind farm in SSO studies," *IEEE Access*, vol. 8, pp. 158380–158390, 2020.

[29] Y. Gu, J. Liu, T. C. Green, W. Li, and X. He, "Motion-induction compensation to mitigate sub-synchronous oscillation in wind farms," *IEEE Trans. Sustain. Energy*, vol. 11, no. 3, pp. 1247–1256, Jul. 2020.

[30] W. Du, B. Ren, H. Wang, and Y. Wang, "Comparison of methods to examine sub-synchronous oscillations caused by grid-connected wind turbine generators," *IEEE Trans. Power Syst.*, vol. 34, no. 6, pp. 4931–4943, Nov. 2019.

[31] H. J. Baesmat and M. Bodson, "Suppression of sub-synchronous resonances through excitation control of doubly fed induction generators," *IEEE Trans. Power Syst.*, vol. 34, no. 6, pp. 4329–4340, Nov. 2019.

[32] J. Khazaei, A. Asrari, P. Idowu, and S. Shushekar, "Sub-Synchronous resonance damping using battery energy storage system," in *Proc. North Amer. Power Symp.*, 2018, pp. 1–6.

[33] T. Rajaram, J. M. Reddy, and Y. Xu, "Kalman filter based detection and mitigation of subsynchronous resonance with SSSC," *IEEE Trans. Power Syst.*, vol. 32, no. 2, pp. 1400–1409, Mar. 2017.

[34] B. Gao and Y. Hu, "Sub-synchronous resonance mitigation by a STATCOM in doubly fed induction generator-based wind farm connected to a series-compensated transmission network," *J. Eng.*, vol. 2019, no. 16, pp. 812–815, 2019.

[35] P. Dattaray, D. Chakravorty, P. Wall, J. Yu, and V. Terzija, "A novel control strategy for subsynchronous resonance mitigation using 11 kV VFD-based auxiliary power plant loads," *IEEE Trans. Power Del.*, vol. 33, no. 2, pp. 728–740, Apr. 2018.

[36] H. A. Mohammadpour and E. Santi, "Modeling and control of gate-controlled series capacitor interfaced with a DFIG-based wind farm," *IEEE Trans. Ind. Electron.*, vol. 62, no. 2, pp. 1022–1033, Feb. 2015.

[37] A. Moharana, R. K. Varma, and R. Seethapathy, "SSR alleviation by STAT-COM in induction-generator-based wind farm connected to series compensated line," *IEEE Trans. Sustain. Energy*, vol. 5, no. 3, pp. 947–957, Jul. 2014.

[38] L. Wang, H. R. Liang, A. V. Prokhorov, H. Mokhlis, and C. K. Huat, "Modal control design of damping controllers for thyristor-controlled series capacitor to stabilize common-mode torsional oscillations of a series-capacitor compensated power system," *IEEE Trans. Ind. Appl.*, vol. 55, no. 3, pp. 2327–2336, May 2019.

[39] X. Wu, M. Wang, M. Shahidehpour, S. Feng, and X. Chen, "Model-Free adaptive control of STATCOM for SSO mitigation in DFIG-based wind farm," *IEEE Trans. Power Syst.*, vol. 36, no. 6, pp. 5282–5293, Nov. 2021.

[40] G. Li, Y. Chen, A. Luo, and H. Wang, "An enhancing grid stiffness control strategy of STATCOM/BESS for damping sub-synchronous resonance in wind farm connected to weak grid," *IEEE Trans. Ind. Informat.*, vol. 16, no. 9, pp. 5835–5845, Sep. 2020.

[41] X. Tian, Y. Chi, Y. Li, H. Tang, C. Liu, and Y. Su, "Coordinated damping optimization control of sub-synchronous oscillation for DFIG and SVG," *CSEE J. Power Energy Syst.*, vol. 7, no. 1, pp. 140–149, Jan. 2021.

[42] B. Shao, S. Zhao, Y. Yang, B. Gao, L. Wang, and F. Blaabjerg, "Nonlinear Sub-synchronous oscillation damping controller for direct-drive wind farms with VSC-HVDC systems," *IEEE J. Emerg. Sel. Topics Power Electron.*, 2020, doi: 10.1109/JESTPE.2020.3025081.

[43] V. Sewdien, R. Preece, J. L. Rueda, and M. A. M. M. Van der Meijden, "Systematic procedure for mitigating DFIG-SSR using phase imbalance compensation," *IEEE Trans. Sustain. Energy*, 2021, doi: 10.1109/TSTE.2021.3104719.

[44] H. Khalilinia, N. Karnik, H. Yin, and M. Sahni, "Power system sub-synchronous oscillation damper," U.S. Patent 9660449, 2017.
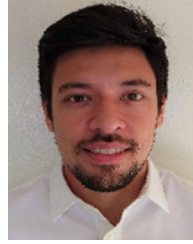
Igor Brandão Machado Matsuo (Student Member, IEEE) received the B.S. and M.S. degrees in electrical engineering from the University of Sao Paulo, Brazil, in 2012 and 2015, respectively.

He held full scholarship from CNPq-Brazil for his Ph.D. degree program from the University of Texas at Arlington, Arlington , TX, USA, where he was a Member of the Energy Systems Research Center. He has also worked for Techimp, the Foundation for the Technological Development of Engineering, and Calpine. His research interests include renewable energy, subsynchronous oscillations, monitoring systems, partial discharges, power system planning and analysis, and automation and protection systems in the generation, transmission, distribution, and industrial levels.

Payman Dehghanian (Senior Member, IEEE) received the B.Sc. degree from the University of Tehran, Tehran, Iran, in 2009, the M.Sc. degree from the Sharif University of Technology, Tehran, in 2011, and the Ph.D. degree from Texas A&M University, College Station, TX, USA, in 2017, all in electrical engineering.

He is currently an Assistant Professor with the Department of Electrical and Computer Engineering, George Washington University, Washington, DC, USA. His research interests include power system reliability and resilience, data-informed decision-making for maintenance and asset management in electrical systems, and smart electricity grid applications.

Dr. Dehghanian is the recipient of the 2014 and 2015 IEEE Region 5 Outstanding Professional Achievement Awards, the 2015 IEEE-HKN Outstanding Young Professional Award, and the 2021 Early Career Award from the Washington Academy of Sciences.

Farshid Salehi (Member, IEEE) received the B.S. degree from Bu-Ali Sina University, Hamedan, Iran, in 2007, the M.S. degree from Semnan University, Semnan, Iran, in 2011, and the Ph.D. degree from the University of Texas at Arlington (UTA), Arlington, TX, USA, in 2018, all in electrical engineering.

He has more than 12 years of academic and industrial experience in power system. He has extensive and in-depth knowledge of electromagnetic transients modeling, renewable technologies, offshore grid design power system planning, and the generation and transmission integrations. He was an Engineer with Monenco Consulting Engineers, a Researcher with Energy System Research Center, UTA. He is currently a Senior Engineer with DNV Energy, Arnhem, The Netherlands. His research interests include power system dynamics and transient stability, arc flash, HVdc systems, power system optimization, and grid integration of the renewable resources.

Mehriar Aghazadeh Tabrizi (Member, IEEE) received the B.S. and M.S. degrees from the Isfahan University of Technology, Isfahan, Iran, in 2005 and 2008, respectively, and the Ph.D. degree from Tennessee Technological University, Cookeville, TN, USA, in 2013, all in electrical power system engineering.

He has more than 16 years of experience in electric grid modeling, planning and compliance including generation/transmission grid integration, reliability, grid code compliance, and detailed modeling of conventional and non-conventional generation units with specific focus on renewable energy and energy storage systems. He is currently the Head of Power System Advisory Department, DNV Energy, Arnhem, The Netherlands.

Dr. Tabrizi is certified as a Professional Engineer in the State of Texas.

Amir Golshani (Member, IEEE) received the Ph.D. degree in electrical engineering with major in power systems from the University of Central Florida, Orlando, FL, USA, in 2017.

He is currently a Senior Engineer with the Power System Advisory Group, DNV Energy, Arnhem, The Netherlands. His research interests include power systems modeling, transient stability and EMT studies, and application of stochastic and robust optimization techniques in power systems, and power systems restoration.

Wei-Jen Lee (Fellow, IEEE) received the B.S. and M.S. degrees from National Taiwan University, Taipei, Taiwan, in 1978 and 1980, respectively, and the Ph.D. degree from The University of Texas at Arlington, Arlington, TX, USA, in 1985, all in electrical engineering.

In 1985, he was with the University of Texas at Arlington, where he is currently a Professor with the Department of Electrical Engineering and the Director of the Energy Systems Research Center. His research interests include power flow, transient and dynamic stability, voltage stability, short circuits, relay coordination, power quality analysis, renewable energy, and deregulation for utility companies.

Dr. Lee is a Registered Professional Engineer with the State of Texas.